Z. Phys. C – Particles and Fields 34, 329–334 (1987)

Zeitschrift für Physik C Particles and Fields

The Process $\gamma+\gamma\to\ell+\ell$ in Coherent Heavy Ion Collisions

G. Alexander[1,2], E. Gotsman[1,2], U. Maor[2]
[1] DESY, D-2000 Hamburg, Federal Republic of Germany
[2] School of Physics and Astronomy, Tel Aviv University, Tel Aviv 69978, Israel

Received 18 December 1986

Abstract. Using a covariant formalism we calculate to leading order the 2-photon contribution to lepton pair production in coherent heavy ion collisions within the framework of EPA. The most significant result of our calculation is the presence of a prominent narrow threshold enhancement in the e^+e^- invariant mass distribution. The position of this peak is essentially energy independent, however, its height and width tend to increase with increasing energy, mass and charge of the colliding ions. Results are presented for configurations at the Bevalac and SPS machines which are then extrapolated down to the GSI energy region.

I. Introduction

Recently, experimental facilities which allow the study of high energy heavy ion collisions became operational, and are producing a large variety of interesting data. In particular the study of lepton pair production in such collisions, has attracted much attention. This interest is triggered in part by the puzzling results, obtained from low energy experiments at the GSI facility [1]. In these experiments e^+e^- pair production is observed which exhibits an exceedingly narrow enhancement very close to threshold. The origin of this peak, which was seen in the collisions of ultra heavy ions with incident kinetic energy of about 6 MeV per nucleon, is at present still unknown. Several hypotheses for its origin have been suggested and a few background sources were investigated [2]. In this paper we discuss in some detail the contribution of the "double Primakoff effect" [3], i.e. we limit our study to coherent production of lepton pairs produced via two quasi-real photons in the process $\gamma\gamma\to e^+e^-$ or $\mu^+\mu^-$.

II. Formalism

In two previous papers [4, 5] we investigated the contribution of the two photon collisions in deep inelastic lepton-nucleon and lepton nucleus scattering. We now extend these calculations to evaluate the cross section for lepton pair production which stem from the $\gamma-\gamma$ reactions in two heavy ion high energy collisions. We restrict ourselves to the double coherent case where we benefit from the kinematics of large mass projectile collisions, as well as from the factor $(Z_1Z_2)^2$, where Z_1 and Z_2 are the charges of the two colliding ions.

We proceed to calculate the two photon contribution to the reaction

$$(A_1,Z_1)+(A_2,Z_2)\to(A_1,Z_1)+(A_2,Z_2)+\ell^+\ell^- \qquad (1)$$

which is illustrated in Fig. 1. The kinematic variables associated with this process are:

$$\begin{aligned} &p_A^2=p_1^2=m_A^2; \quad p_B^2=p_3^2=m_B^2;\\ &p_2^2=(q_1+q_2)^2=W_{\gamma\gamma}^2=m_{\ell^+\ell^-}^2;\\ &q_1^2=-Q^2; \quad q_2^2=-P^2. \end{aligned} \qquad (2)$$

In addition we define:

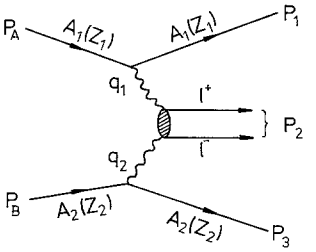

Fig. 1. Diagram for the $\gamma\gamma$ process in two ion collisions

$$s=(p_A+p_B)^2;$$
$$W_A^2=(q_2+p_A)^2; \quad W_B^2=(q_1+p_B)^2; \tag{3}$$
$$\omega_1=q_1\cdot(p_A+p_B)/\sqrt{s}; \quad \omega_2=q_2\cdot(p_A+p_B)/\sqrt{s}.$$

$$F'=\frac{[(W_{\gamma\gamma}^2+Q^2+P^2)^2-4Q^2P^2]^{1/2}}{[(s-m_A^2-m_B^2)^2-4m_A^2m_B^2]^{3/2}}$$

where σ_{TT} stands for the transverse photon-photon cross section $\gamma(Q^2)+\gamma(P^2)\to\ell^+\ell^-$ and

$$2\rho_A^{++}=\left[1+\frac{W_{\gamma\gamma}^2+Q^2+P^2}{(W_{\gamma\gamma}^2+Q^2+P^2)^2-4Q^2P^2}\right]C_A$$
$$+\left[\frac{(4\sqrt{s}\,\omega_2+2P^2)^2-2(4\sqrt{s}\,\omega_2+2P^2)(W_{\gamma\gamma}^2+Q^2+P^2)}{2\{(W_{\gamma\gamma}^2+Q^2+P^2)^2+4Q^2P^2\}}-\frac{2m_A^2}{Q^2}\right]D_A \tag{5}$$

Our notation is essentially the same as that of Budnev et al. [6], where ω_1 and ω_2 denote the energy transfers associated with Q^2 and P^2 in the center of mass system. The 2-photon exchange cross section corresponding to the diagram shown in Fig. 1 provides the leading contribution to the lowest order calculation, as long as $Z_1Z_2\alpha^2\ll1$ and other diagrams of this order can be neglected. It has been shown [7] that competing processes, most notably the bremsstrahlung channels with a timelike photon, are much smaller than the 2-photon exchange contribution discussed here. Approximate evaluations of Fig. 1 were made sometime ago by the authors of [6, 8]. In our covariant formulation the only approximation used is the Equivalent Photon Approximation (EPA) [9] which can be applied over the whole range of kinematic variables. The EPA simplifies the calculation and is justified as the main contribution to our integrals come from Q^2 and P^2 region near the lower kinematic bounds which are indeed very small for the cases treated below. For example in the reaction $O+Pb\to O+Pb+(e^+e^-)$, $Q^2_{\min}=0.132\times10^{-3}$ GeV^2, for incident kinetic energy of 8 MeV/nucleon and this decreases to $Q^2_{\min}=0.103\times10^{-7}$ GeV^2, for $E_{K/A}=15$ GeV.

The cross section for the process illustrated in Fig. 1 can be expressed as [6]:

$$d\sigma=\frac{\alpha^2}{4\pi^4\,q_1^2\,q_2^2}\left[\frac{(q_1\cdot q_2)^2-q_1^2\,q_2^2}{(p_A\cdot p_B)^2-m_A^2\,m_B^2}\right]^{1/2}$$
$$\cdot\rho_A^{++}\,\rho_B^{++}\,\sigma_{TT}\,\frac{d^3p_1}{E_1}\,\frac{d^3p_3}{E_3}. \tag{4}$$

This can be rewritten in terms of more convenient variables as

$$d\sigma=\frac{\alpha^2 s}{4\pi^2Q^2P^2}\,F'\,\rho_A^{++}\,\rho_B^{++}\,\sigma_{TT}$$
$$\cdot dQ^2\,dP^2\,d\omega_1\,d\omega_2\left(\frac{d\phi}{2\pi}\right) \tag{4'}$$

with

for $2\rho_B^{++}$ one has the same expression with the substitutions: $A\leftrightarrow B$, $Q^2\leftrightarrow P^2$, $\omega_2\leftrightarrow\omega_1$. The appropriate nuclear form factors are given by:

$$C_i(Z=1)=G_M^2(q_i^2); \quad C_i(Z>1)=0$$
$$D_i(Z=1)=F_p^2(q_i^2); \quad D_i(Z>1)=Z^2F_c^2(q_i^2) \tag{6}$$

with

$$G_M(q_i^2)=2.79\,G_E(q_i^2)$$
$$G_E(q_i^2)=[1-q_i^2/0.71\ \text{GeV}^2]^{-2}$$
$$F_p^2(q_i^2)=(4m_p^2\,G_E^2-q_i^2\,G_M^2)/(4m_p^2-q_i^2) \tag{7}$$
$$F_c^2(q_i^2)=[1-q_i^2\langle2r_i^2\rangle]^{-4}.$$

The expression used for the electric form factor is identical to that which we used in a previous paper [5] and was discussed in detail there. In the numerical calculation of (4') we average over the azimuthal angle ϕ, and calculate $d\sigma/dW_{\gamma\gamma}^2$. The relevant limits of integration for $d/dW_{\gamma\gamma}^2$ are

$$\omega_1^{\min}=\frac{1}{2\sqrt{s}}[(m_B+W_{\gamma\gamma})^2-m_B^2];$$
$$\omega_1^{\max}=\frac{1}{2\sqrt{s}}[(\sqrt{s}-m_A)^2-m_A^2]. \tag{8}$$

For Q^2 we have

$$Q^{2\,\max}_{\min}=-m_A^2-m_1^2+\frac{1}{2s}(s+m_A^2-m_B^2)(s+m_A^2-W_B^2)$$
$$\pm\frac{1}{2s}[\lambda(s,m_A^2,m_B^2)\,\lambda(s,m_1^2,W_B^2)]^{1/2}. \tag{9}$$

For P^2 they are

$$P^{2\,\max}_{\min}=Q^2-W_{\gamma\gamma}^2+\frac{1}{2W_B^2}$$
$$\cdot(W_B^2-Q^2-m_B^2)(W_B^2+W_{\gamma\gamma}^2-m_B^2)$$
$$\pm\frac{1}{2W_B^2}[\lambda(W_B^2,-Q^2,m_B^2)$$
$$\cdot\lambda(W_B^2,W_{\gamma\gamma}^2,m_B^2)]^{1/2} \tag{10}$$

where

$$\lambda(x, y, z)=x^2+y^2+z^2-2(xy+xz+yz).$$

Note that

$$\omega_2=\frac{(W_A^2-m_A^2)}{2\sqrt{s}}$$

where

$$W_A^2=s+m_B^2-T/\lambda(W_B^2, -Q^2, m_B^2)$$

$$T=\det\begin{vmatrix} 2m_B^2 & W_B^2+Q^2+m_B^2 & 2m_B^2+P^2 \\ W_B^2+Q^2+m_B^2 & 2W_B^2 & W_B^2-W_{\gamma\gamma}^2+m_B^2 \\ s-W_A^2+m_B^2 & s+W_B^2-m_A & 0 \end{vmatrix}$$

Our final expression can thus be written

$$\frac{d\sigma}{dW_{\gamma\gamma}^2}=\iiint F\sigma_{\gamma\gamma}(W_{\gamma\gamma}^2, Q^2, P^2)\cdot f_A f_B\, d\omega_1\, dQ^2\, dP^2 \qquad (11)$$

where

$$F=2\cdot sF'\left[\omega_1+\omega_2\left\{\frac{(\omega_1^2+Q^2)}{(\omega_2^2+P^2)}\right\}^{1/2}\cos\theta_{1,2}\right]$$

$$\cos\theta_{1,2}=\frac{W_{\gamma\gamma}^2+Q^2+P^2-2\omega_1\omega_2}{2[(\omega_1^2+Q^2)(\omega_2^2+P^2)]^{1/2}}$$

$$f_A=\frac{\alpha}{2\pi Q^2}\rho_A^{++};\quad f_B=\frac{\alpha}{2\pi P^2}\rho_B^{++}.$$

III. Results

We present our results for various configurations which are of practical interest. These were chosen so that the parameters correspond to the experimental facilities which presently exist at the Bevalac, and at the SPS at CERN. In Figs. 2 and 3 we display the differential cross section $d\sigma/dm_{\ell\ell}^2$ as a function of $m_{\ell\ell}^2$ for the reactions

$$Fe^{26}+Fe^{26}\to Fe^{26}+Fe^{26}+(e^+e^-)$$
$$Fe^{26}+Fe^{26}\to Fe^{26}+Fe^{26}+(\mu^+\mu^-)$$
$$O^{16}+Pb^{204}\to O^{16}+Pb^{204}+(e^+e^-)$$
$$O^{16}+Pb^{204}\to O^{16}+Pb^{204}+(\mu^+\mu^-)$$

at kinetic energies of $E_k=1.88$ and 15 GeV per nucleon. The effect of the nuclei mass on the cross section can be seen by comparing the above results with the reaction

$$U^{238}+U^{238}\to U^{238}+U^{238}+(e^+e^-)$$
$$U^{238}+U^{238}\to U^{238}+U^{238}+(\mu^+\mu^-)$$

at $E_k=1.88$ GeV per nucleon (Fig. 4).

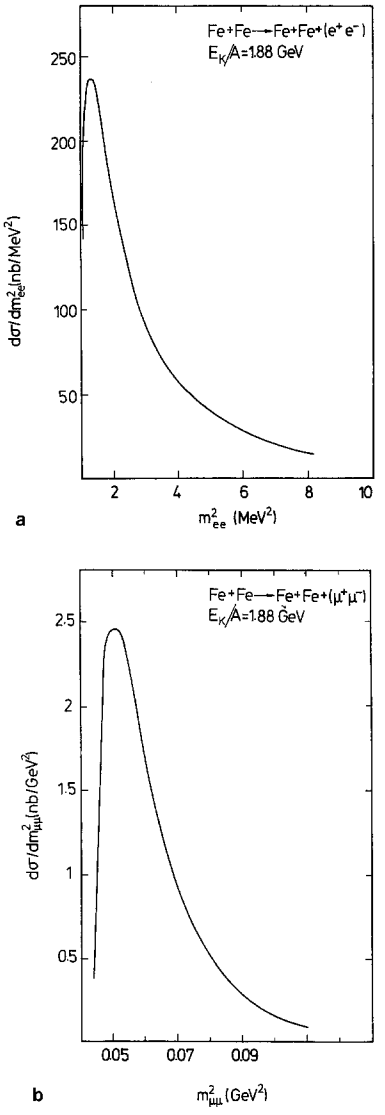

Fig. 2a, b. $d\sigma/dm^2$ for the reaction $Fe+Fe\to Fe+Fe+(\ell\ell)$ for incident kinetic energy of 1.88 GeV per nucleon. **a** $\ell\ell=e^+e^-$; **b** $\ell\ell=\mu^+\mu^-$

In comparing Figs. 2–4 we note the following general features, which pertain to all three processes:

a) The distributions exhibit a threshold peak very close to the value $4m_{\ell\ell}^2$, its position is almost independent of the energy and type of colliding ions.

b) The width of the peak, which is rather narrow (about 1.2 MeV^2 for (e^+e^-) pairs) at low incident energies becomes broader when the incident kinetic energy is increased to several GeV per nucleon.

c) For a given process, an increase in the kinetic energy of the incoming ion gives rise to an increase in the magnitude of the differential cross section.

d) The large difference in magnitude in the differential cross sections for the production of (e^+e^-) and

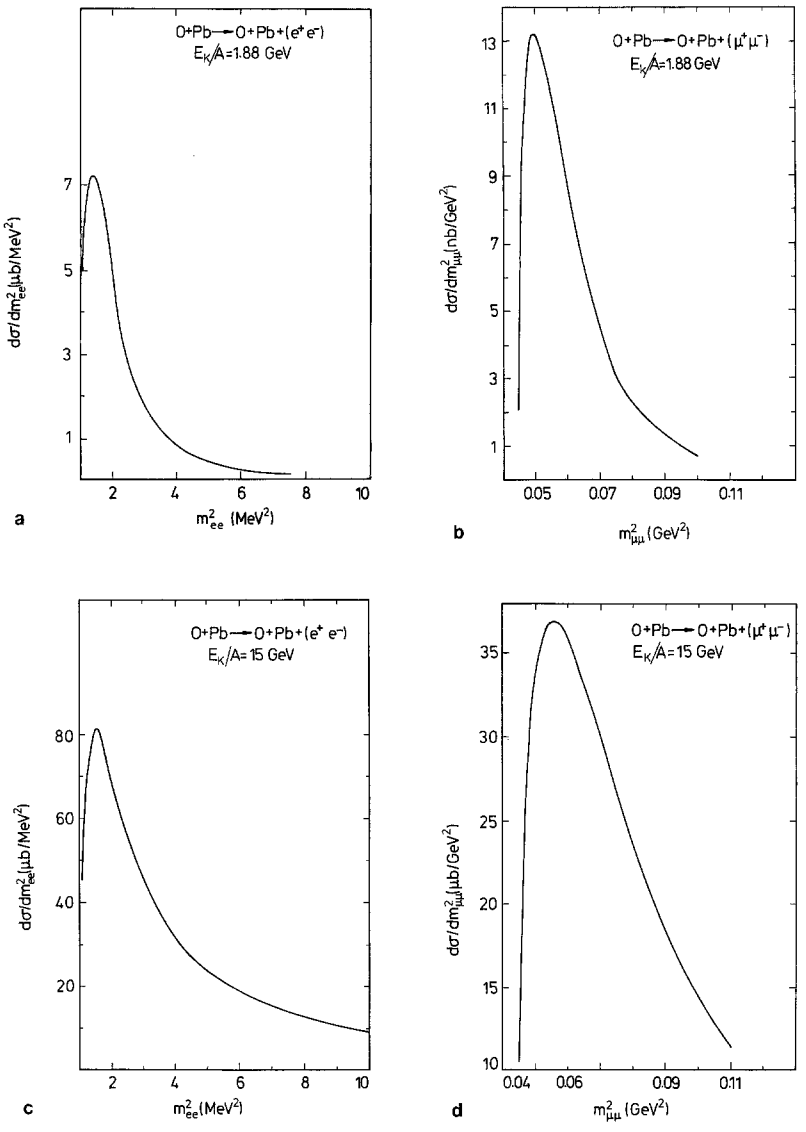

Fig. 3a–d. $d\sigma/dm^2$ for the reaction $O+Pb\to O+Pb+(\ell\ell)$ for incident kinetic energy of 1.88 and 15 GeV per nucleon. **a** and **c** for electron pairs; **b** and **d** for muon pairs

$(\mu^+\mu^-)$ pairs under the same conditions, is due to the different mass thresholds, and consequently different $Q^2_{\min}$ pertaining to the two processes.

Additional properties of the 2γ process in heavy ion collisions cannot readily be deduced from (4) or (4′) without detailed numerical calculations, since the kinematic factors in the above expressions have a non trivial dependence on the masses and energies of the colliding ions. For a given reaction, an increment in the kinetic energy of the projectile increases the ion's incoming flux and, consequently one would expect a smaller cross section. However, this also causes a decrease in the lower kinematic bounds of the integration (over P^2 and Q^2) resulting in an overall increase in the differential cross section. An additional complicating factor when comparing the results of the different reactions is the non linear dependence between the charges and masses of the different ions.

As the SPS accelerator at CERN is set to accelerate light ions to energies of 200 GeV/nucleon, we have calculated the cross section for the process

$$O^{16}+Pb^{204}\to O^{16}+Pb^{204}+(\mu^+\mu^-)$$

at this energy. The results are shown in Fig. 5. We note that at this energy the position of the peak has moved to slightly higher mass squared values and has become much broader. The magnitude of the peak of the differential cross section is a factor of a hundred larger than for $E_{K/A}=15$ GeV. (Compare Figs. 3d and 5.)

The cross sections at high energy and fixed mass increase like $\ln^2(s)$ as expected (see Fig. 6). It should be mentioned, that, following the methods described in [4, 5] one can easily extend our calculations

a) to include the non-coherent 2-photon process,

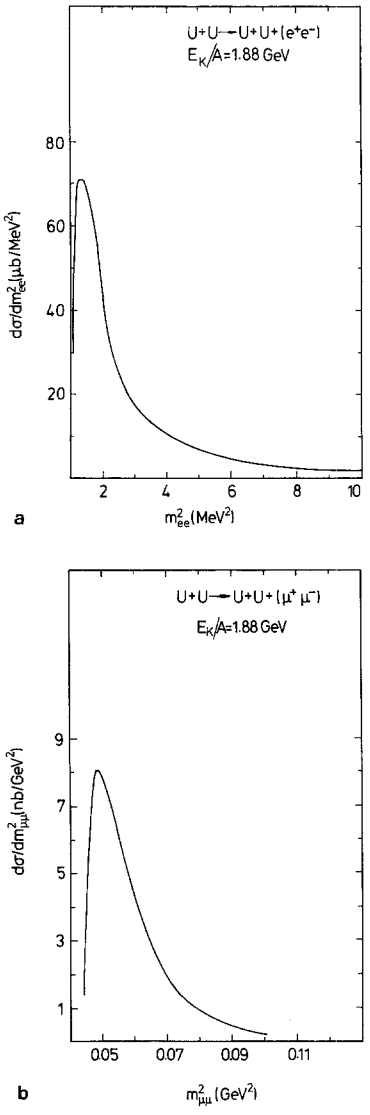

Fig. 4a, b. $d\sigma/dm^2$ for the reaction $U+U\to U+U+(\ell\ell)$ for incident kinetic energy of 1.88 GeV per nucleon. **a** for electron pairs; **b** for muon pairs

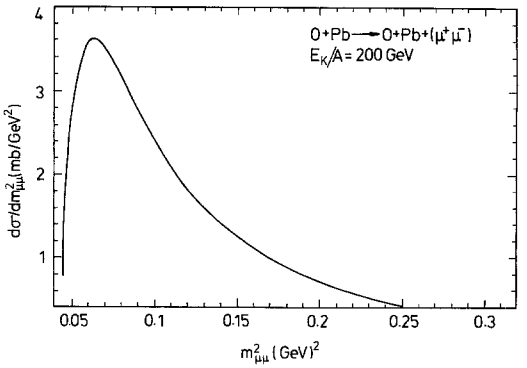

Fig. 5. $d\sigma/dm^2_{\mu\mu}$ for the reaction $O+Pb\to O+Pb+(\mu^+\mu^-)$ for incident kinetic energy of 200 GeV per nucleon

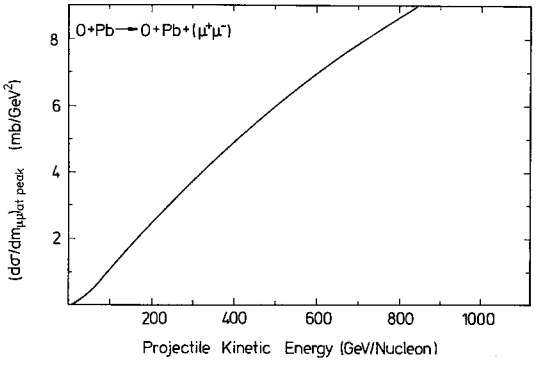

Fig. 6. $d\sigma/dm^2_{\mu\mu}$ at peak as a function of centre of mass energy squared s for the reaction $O+Pb\to O+Pb+(\mu^+\mu^-)$

and

b) estimate the hadron production in these processes. The production of a lepton pair by the 2-photon process is however, far easier to detect experimentally.

It is also of interest to investigate the e^+e^- production process at energies of several MeV per nucleon, as long as $Z_A Z_B \alpha^2 \ll 1$. In Fig. 7a we show our results for $Fe+Fe\to Fe+Fe+(e^+e^-)$ with $E_K = 8$ MeV per nucleon. The $d\sigma/dm^2_{ee}$ exhibits a sharp enhancement at $m^2_{ee}=1.4$ MeV^2 with a peak cross section of 0.59 nb/MeV^2 and an approximate full width of 1.3 MeV^2.

To study the role of the charge of the nuclei on the size of the 2-photon cross section we have also calculated e^+e^- pair production in the reaction $O+Pb\to O+Pb+(e^+e^-)$ Fig. 7b. This process has an additional advantage in that the product of its charges (8×82) is practically identical to the product of charges of Fe+Fe (i.e. 26×26), enabling one to isolate the dependence of the ion masses on the cross section. The shapes of $d\sigma/dm^2_{ee}$ for the three reactions are very similar (see Fig. 7) while the cross sections for the electron pair production at E_K of 8 MeV per nucleon are in the ratio of approximately 65:228:600 for Fe+Fe, O+Pb and U+U.

In view of the recent results at GSI [1], where a (e^+e^-) sharp enhancement has been observed to be produced with a cross section of several μb in very heavy ion collisions, we also show our results for the reaction $U+U\to U+U+(e^+e^-)$ at $E_k = 8$ MeV per nucleon (Fig. 7c). Bearing in mind that for this process, with very high Z ions, other diagrams with multi-photons may no longer be negligible [10]. On the other hand, it is not unreasonable to assume that the main features of the reaction will still be

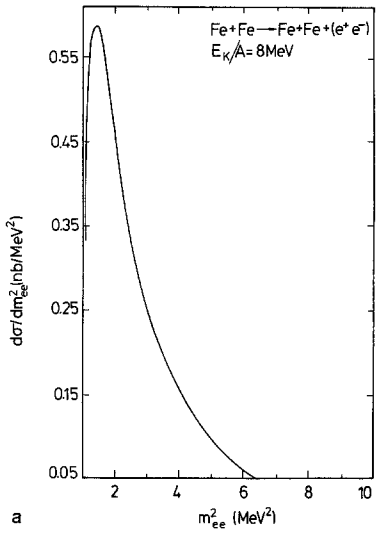

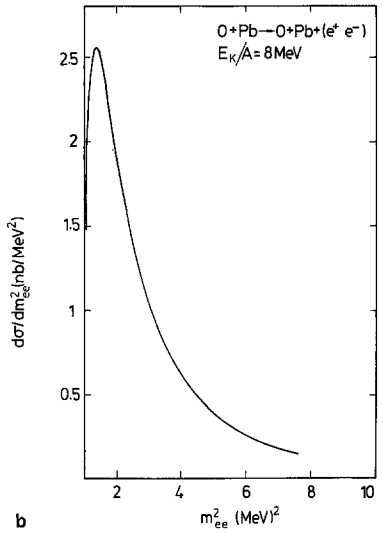

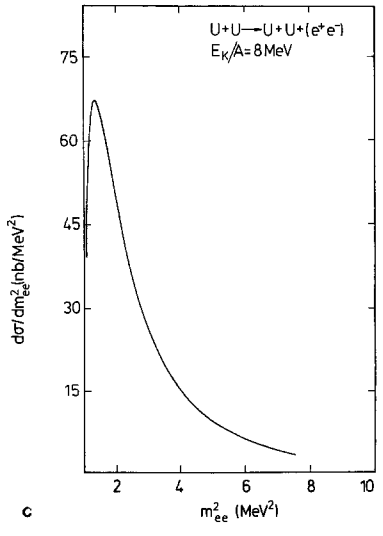

Fig. 7a–c. The $d\sigma/dm_{ee}^2$ production cross section for e^+e^- pairs in the reactions. **a** Fe+Fe; **b** O+Pb; **c** U+U at incident kinetic energy of 8 MeV per nucleon

approximately given by the 2-photon process shown in Fig. 1. As in the case of Fe+Fe collisions a narrow prominent peak is seen in $d\sigma/dm_{ee}^2$ distribution attaining a maximum of 68 nb/MeV^2 at a mass squared value of 1.3 MeV^2. To compare our results with the GSI effect, we integrate the distribution over m_{ee}^2 and obtain a total cross section for the 2 photon produced (e^+e^-) peak of about 126 nb. This value is appreciably smaller than the current reported cross section value for the GSI effect.

IV. Conclusions

We have calculated a sizeable and kinematically well located contribution to lepton pair production in high energy heavy ion collisions. This contribution should be experimentally detectable and can supplement the study of gamma-gamma reactions in electron colliders. Furthermore the $\gamma\gamma$ process should be included in the evaluation of background to relevant processes in heavy ion collisions. In particular we emphasize the need to properly evaluate this and similar electromagnetic background contributions to the low energy GSI experiments.

Acknowledgements. We would like to thank D. Ashery, J. Eisenberg, W. Greiner, R. Peccei and D. Schwalm for many helpful discussions. Part of this work was done while G.A. and E.G. were visiting DESY. They would like to thank the DESY directorate for their kind hospitality and the MINERVA foundation for its financial support.

References

1. J. Schweppe et al.: Phys. Rev. Lett. **51**, 2261 (1983); M. Clemente et al.: Phys. Lett. **137B**, 41 (1984); T. Cowan et al.: Phys. Rev. Lett. **54**, 1761 (1985); **56**, 444 (1986); H. Tsertos et al.: Phys. Lett. **162B**, 372 (1985)
2. Some recent theoretical works are J. Reinhardt et al.: Phys. Rev. **C33**, 194 (1986); B. Müller et al.: J. Phys. **G12**, L109 (1986); R.D. Peccei et al.: DESY report 86–013 (to be published); A. Schäfer et al.: GSI Preprint, 86–12
3. H. Primakoff: Phys. Rev. **81**, 899 (1951)
4. G. Alexander, E. Gotsman, U. Maor: Phys. Lett. **161B**, 384 (1985)
5. G. Alexander, E. Gotsman, U. Maor: Z. Phys. C – Particles and Fields **32**, 105 (1986)
6. V.M. Budnev, I.F. Ginzburg, G.V. Serbo: Phys. Rep. **C15**, 181 (1975)
7. See e.g. V. Barger et al.: Phys. Rev. **D20**, 630 (1979)
8. C. Carimalo, P. Kessler, J. Parisi: College de France preprint L.P.C. 81–30, (unpublished)
9. C.F. v. Weizsäcker: Z. Phys. **88**, 612 (1934); E.J. Williams: Proc. Roy. Soc. Lond. **A139**, 169 (1933); Phys. Rev. **45**, 729 (1934); L. Landau, E. Lifshitz: Phys. Z. Soviet Union **6**, 244 (1934); P. Kessler: Nuovo Cimento **17**, 809 (1960)
10. See e.g., W. Greiner, B. Müller, J. Rafelski: Quantum electrodynamics of strong fields. Berlin, Heidelberg, New York: Springer 1985